JOURNAL OF GEOPHYSICAL RESEARCH, VOL. 95, NO. A2, PAGES 1103–1111, FEBRUARY 1, 1990

Continuum Radiation at Uranus

W. S. KURTH AND D. A. GURNETT

Department of Physics and Astronomy, University of Iowa, Iowa City

M. D. DESCH

Laboratory for Extraterrestrial Physics, NASA Goddard Space Flight Center, Greenbelt, Maryland

Uranus has proven to be a radio source of remarkable complexity with as many as six distinctly different types of emission. One Uranian radio emission which has thus far escaped attention is an analog of continuum radiation at Earth, Jupiter, and Saturn. The emission is found to be propagating in the ordinary mode in the range of one to a few kHz on the inbound leg of the Voyager 2 encounter, shortly after the magnetopause crossing. The continuum radiation spectrum at Uranus also includes bands with frequencies as high as 12 kHz or greater on both the inbound and outbound legs. The Uranian continuum radiation is notably weak, making it more like that detected at Saturn than the extremely intense Jovian continuum radiation. The Uranian emission shows some evidence for narrow-band components lying in the same frequency regime as the continuum, completing the analogy with the other planets, which also show narrow-band components superimposed on the continuum spectrum. We argue that the low intensity of the Uranian continuum is most likely related to the lack of a density cavity within the Uranian magnetosphere that is deep relative to the solar wind plasma density.

1. INTRODUCTION

The Voyager 2 encounter with Uranus revealed that the magnetosphere of the planet is a rich source of radio emissions [*Warwick et al.*, 1986]. By some counts, there are six separate types of radio sources at Uranus [*Leblanc et al.*, 1987; *Desch and Kaiser*, 1987; *Kurth et al.*, 1986]. This paper presents an additional component of the Uranian radio spectrum at very low frequencies, referred to here as continuum radiation in analogy with similar emissions observed at the Earth [*Gurnett*, 1975], Jupiter [*Scarf et al.*, 1979], and Saturn [*Kurth et al.*, 1982]. The Uranian continuum radiation was mentioned very briefly by *Gurnett et al.* [1986], but details of its occurrence, spectrum, and generation have not been reported heretofore.

The Uranian continuum radiation lies in a frequency range of 1–3 kHz, trapped in the density cavity between the magnetopause and the dense inner magnetosphere. The emission is remarkable not for its intensity, since its peak power flux is only about 3×10^{-16} W/(m^2 Hz), but because of the ubiquity of this type of emission in planetary magnetospheres. All planetary magnetospheres investigated to date with appropriate wave sensors exhibit the emission.

In addition to the 1- to 3-kHz component, we will also discuss similar emissions that are detected in the Voyager wideband receiver at frequencies above about 6 kHz. The source of this higher-frequency emission is not as obvious as for the 1- to 3-kHz component. We will discuss a few possibilities for the source of the higher-frequency emissions and will conclude that the higher-frequency emissions are probably generated by the same mechanism as the 1- to 3-kHz emission.

The observations used herein are from the Voyager 2 plasma wave receiver described by *Scarf and Gurnett* [1977] and from the planetary radio astronomy receiver described by *Warwick et al.* [1977]. The most definitive measurements for the detection of the continuum radiation are from the wideband waveform receiver of the plasma wave instrument, which has a passband of about 40 Hz to 12 kHz. The electric field waveform in this frequency range is digitized to 4-bit resolution at a rate of 28,800 samples per second. These waveforms are Fourier transformed in order to produce frequency-time spectrograms on the ground with resolution limited only by the Fourier transform, $\Delta f \Delta t \simeq 1$; that is, spectral resolution may be gained by transforming longer intervals of time and hence sacrificing temporal resolution, or vice versa.

The other portion of the plasma wave instrument is a spectrum analyzer covering the range from 10 Hz to 56 kHz with 16 logarithmically spaced channels. In the frequency range of interest here, i.e., $\geq$1 kHz, the spectrum analyzer data are degraded due to a failure in the spacecraft data system that occurred shortly after launch. The failure results in decreased sensitivity in the $\geq$1-kHz channels and a less reliable calibration for the same channels.

The planetary radio astronomy receiver measures the amplitudes of waves in the frequency range of 1.2 kHz to 40.5 MHz. Of interest to this study is the 1.2-kHz channel, which has a bandwidth of 1 kHz. Right-hand (RH) and left-hand (LH) circular polarizations are measured alternately, enabling us to make some conclusions about the sense of polarization of received signals.

Finally, Voyager has only an electric dipole antenna; no magnetic signature is measured for waves. Hence conclusions as to the electrostatic or electromagnetic nature of waves must be drawn on the basis of the frequency spectrum, which gives information on the mode of propagation, or on the temporal variability of the emission (electrostatic emissions tend to be much more sporadic than electromagnetic waves), and on the basis of analogies with terrestrial emissions for which the electric-to-magnetic field ratio has

Paper number 89JA00872.
0148-0227/90/89JA-00872$02.00

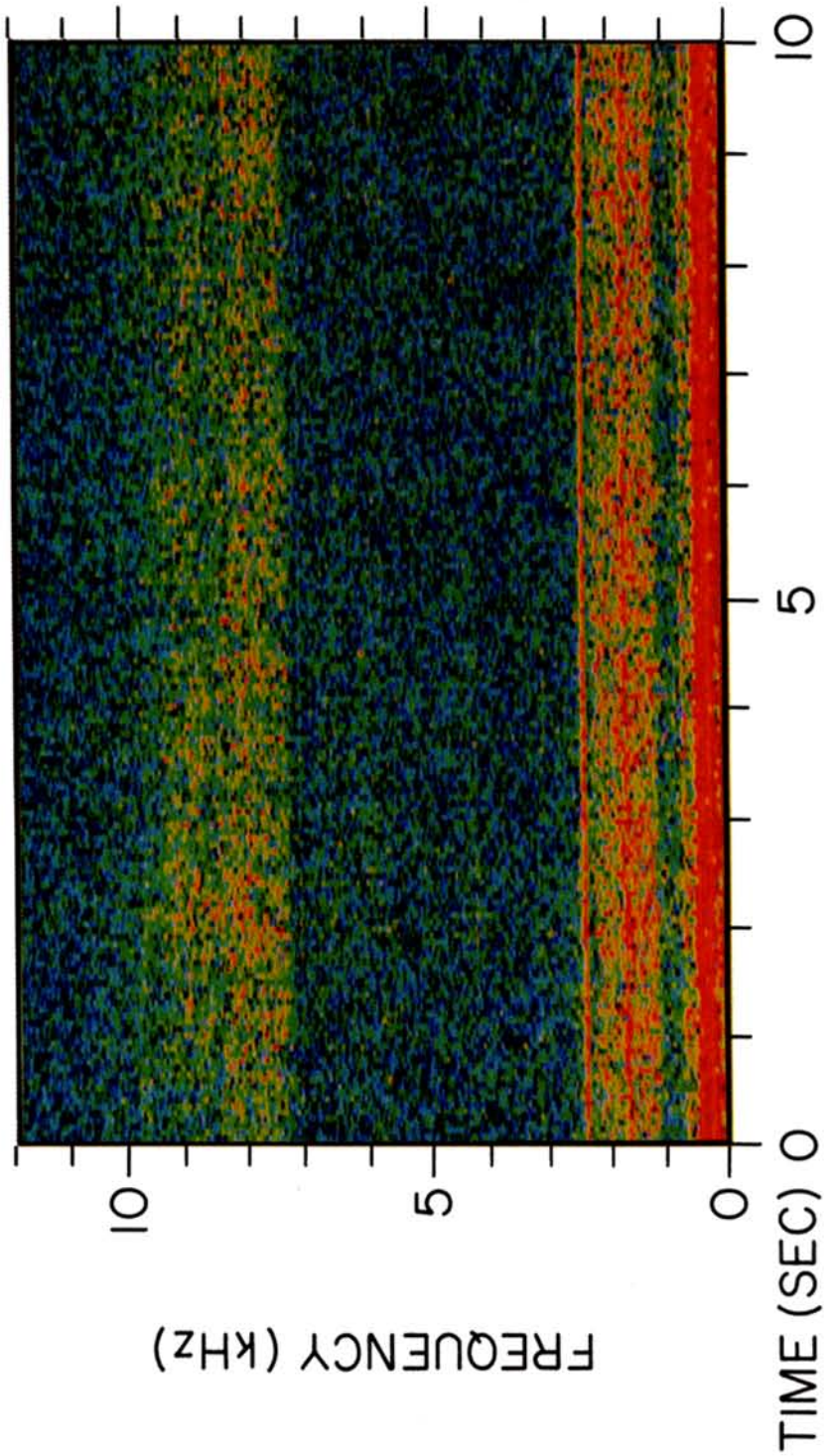

Plate 1. Frequency-time spectrogram showing a band of trapped continuum radiation between about 1 and 2.3 kHz as well as a second band of similar emission above 7 kHz. Note that the spectrum shows almost no variation over time in this 10-s interval.

been measured. Fortunately, the planetary radio astronomy receiver can measure the polarization of electromagnetic waves by using the two elements of the electric antenna as monopoles and noting the phase of the detected signal. As will be seen, this information allows a comparison with theoretical predictions on the polarization of the continuum radiation and leaves little doubt about the mode of the 1- to 3-kHz signal.

2. OBSERVATIONS

2.1. *The 1- to 3-kHz Emission*

In this section we describe the observations of the Uranian continuum radiation observed on the inbound (dayside) leg of the encounter. Plate 1 and Figure 1 detail many of the characteristics of the emission. Plate 1 is a frequency-time spectrogram from the wideband receiver that shows the amplitudes of waves as a function of frequency (ordinate) and time (abscissa). The most intense waves are represented as red, and the weakest as blue.

The feature of interest in Plate 1 is the band lying between about 1 and 2.3 kHz. The narrow-band tone at 2.4 kHz is interference from the spacecraft power supply, and the narrow-band line at about 1.7 kHz is also thought to be an interference effect, although the source is unknown. The 1.7-kHz line has appeared occasionally as early as the Saturn encounter with no apparent relation to local plasma conditions; hence it seems unlikely to be a natural emission.

The emission between 1 and 2.3 kHz is generally featureless, exhibiting little variation in either time or frequency. These are the characteristic features of continuum radiation at other planets, although narrow-band features can sometimes be observed. Figure 1 is a plot of amplitude versus frequency obtained by averaging over the 10-s interval of data displayed in Plate 1 and shows, besides the probable interference line at 1.7 kHz, some fluctuations in amplitude across the band. One aspect of continuum radiation at the other planets [cf. *Kurth et al.*, 1982] that is not apparent in the spectrum in Figure 1 is a power law spectrum. Typical continuum radiation spectra from Earth have amplitudes that vary as $f^{-\alpha}$ where α varies between 3 and 6 [*Kurth et al.*, 1982]. The spectrum in Figure 1 appears to be roughly flat up to 2.3 kHz and has an abrupt cutoff. This cutoff could be due, in part, to the notch filter at 2.4 kHz designed to limit the power supply interference.

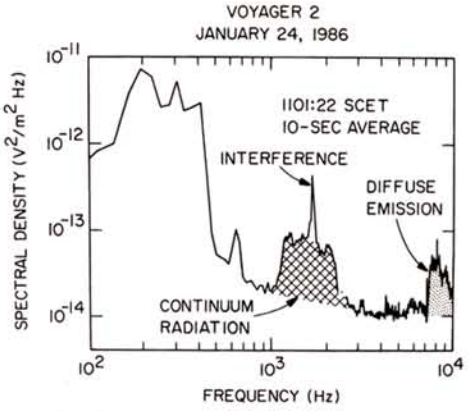

Fig. 1. Plot of electric field spectral density as a function of frequency for the data shown in Plate 1. Note that the trapped continuum band just above 1 kHz shows some weak evidence for narrow-band features and a relatively sharp upper frequency cutoff. There is further evidence for radio emissions above 7 kHz with a spectrum which decreases in amplitude with increasing frequency.

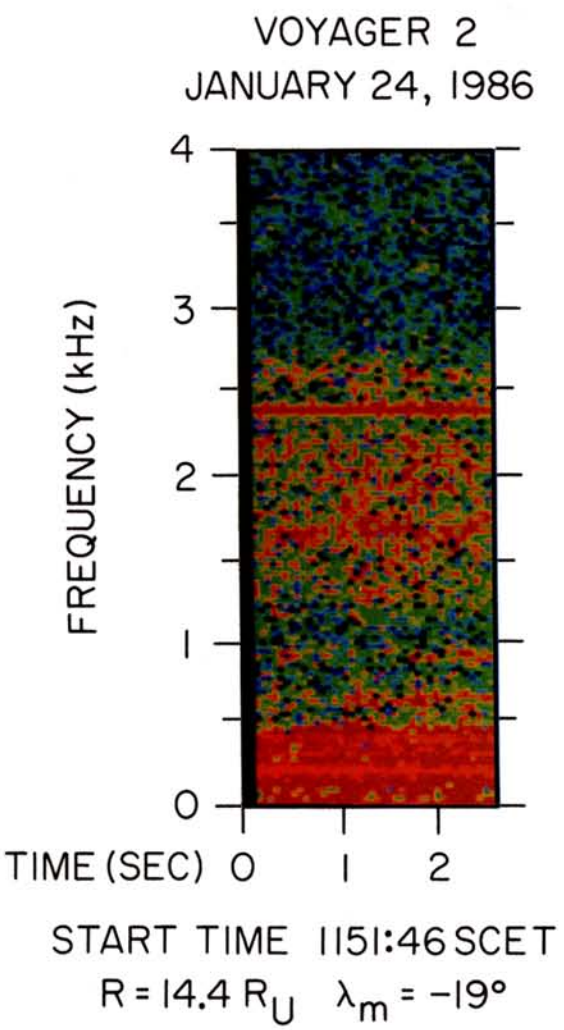

Plate 2. Second example of trapped continuum radiation demonstrating that the band shown in Plate 1 is present in almost identical form almost an hour later.

Plate 2 is another frequency-time spectrogram which shows the temporal invariability of the emission; this frame is separated by almost an hour in time from the example in Plate 1 and by more than 1 R_U (one Uranian radius), spatially. The interval shown in Plate 2 is limited by intense interference in the remainder of the frame caused by a stepper motor on board the spacecraft. The basic features of the emission in Plate 2 are the same as those in Plate 1, except that the upper frequency limit has shifted to about 2.7 kHz. The amplitude spectrum in Figure 2 verifies that there are only minor changes, although the spectrum is noisier owing to a decreased averaging interval (2.3 s versus 10 s in

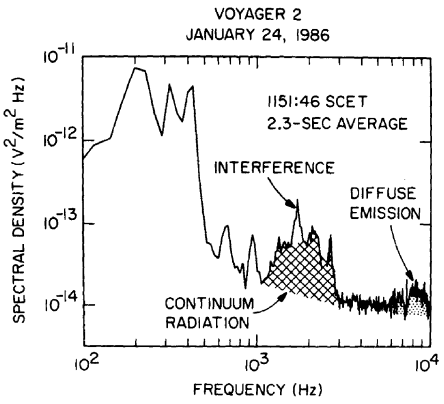

Fig. 2. Plot of spectral density versus frequency for the spectrogram taken at about 1152 SCET showing features very similar to those in Figure 1.

Figure 1). The similarity between these widely spaced observations and the very stable temporal character, even on 1-s time scales, suggest that the emission is a propagating radio emission since a localized plasma emission would likely show greater variations. Also, the electron density measured by the plasma instrument in this region of the magnetosphere is about 2×10^{-3} cm^{-3} [*Sittler et al.*, 1987], which gives a plasma frequency of only about 400 Hz. The electron cyclotron frequency is less than about 300 Hz based on Voyager magnetometer measurements. Hence we conclude that the emission must be free space electromagnetic radiation, since the wave frequency is greater than any of the characteristic frequencies of the plasma.

For the inbound leg of the Uranus encounter the data presented in Figures 1 and 2 and Plates 1 and 2 constitute the sum total of the wideband observations showing the 1- to 3-kHz continuum radiation. We can supplement these high-resolution data with the continuously available spectrum analyzer data as shown in Figure 3. Figure 3 shows the electric field spectral density from six of the spectrum analyzer channels ranging in frequency from 562 Hz to 10 kHz. It is this type of display which enabled *Gurnett et al.* [1986] to initially identify the existence of the continuum radiation. The increase in signal strength in the 1.78-kHz channel shortly after 1000 spacecraft event time (SCET) occurs simultaneously with the crossing of the magnetopause and hence the passage of the spacecraft into the low-density cavity of the magnetosphere. *Gurnett et al.* [1986] used this feature as an indication of the low-frequency radio waves trapped within the cavity. The increase in intensity in the 1-kHz channel just prior to 1100 SCET represents the extension of the continuum spectrum into the passband of the 1-kHz channel. We should note that care must be taken in interpreting step-level changes in the Voyager 2 spectrum analyzer data at or above 1 kHz since the failure in the spacecraft data system may be a cause of such features. The changes caused by the failure tend to affect two or more channels simultaneously as for the $\sim\frac{1}{2}$-hour interval just prior to 1400. We have a high degree of confidence in the validity of the increase near 1008 SCET because it occurs only at 1.78 kHz and because of its relationship with the magnetopause crossing.

We have tried to summarize the various pieces of evidence

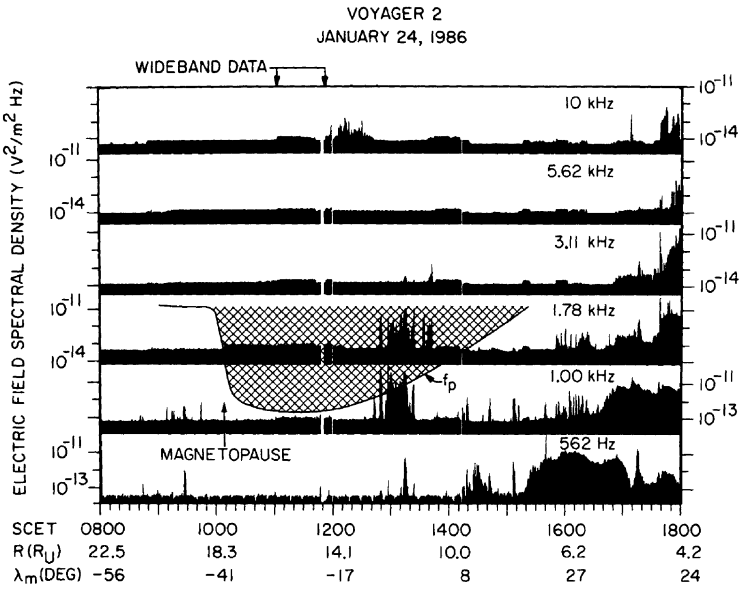

Fig. 3. Display of the spectrum analyzer data relevant to the trapped continuum radiation shown in Figures 1 and 2 and Plates 1 and 2. The bursty emissions centered around 1315 SCET are Bernstein waves which are thought to be the source of the trapped continuum radiation. The lower bound of the cross-hatched region showing the extent of the continuum radiation is an upper limit to the electron plasma frequency based on the lower frequency cutoff of the continuum radiation.

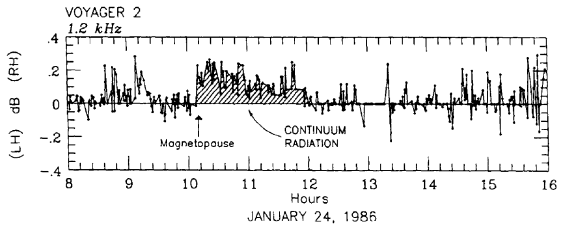

Fig. 4. Plot showing the intensity versus time of emission recorded at 1.2 kHz from the planetary radio astronomy experiment on Voyager. The intensity (decibels) is displayed in terms of the net polarized signal (RH − LH) so that RH (LH) polarized emission is positive (negative). The continuum radiation starts abruptly at the time of magnetopause crossing and ends around 1205 SCET. The continuum emission is observed to be exclusively RH polarized (in the radio astronomy sense [*Kraus*, 1966]), consistent with *L-O* mode waves generated in the magnetic equator and propagating toward Voyager approximately antiparallel (or, at an obtuse angle) to the local magnetic field.

for the trapped continuum radiation by the addition of the cross-hatched region in Figure 3. The lower bound of the region is an estimate of the local plasma frequency (related to the electron density by $f_p = 9000(n_e)^{1/2}$ where f_p is in hertz and n_e is the electron density in cm^{-3}) obtained by assuming the continuum cutoff is at f_p. We have used the increase in intensity at the magnetopause at 1.78 kHz and the lower frequency cutoff of the continuum radiation in the two wideband frames in Figures 1 and 2 for guidance in drawing the f_p contour. Actually, the continuum cutoff is an upper limit for f_p; as mentioned above, the plasma instrument's measurement of the density is consistent with $f_p \simeq 400$ Hz. We have also used a plasma frequency derived from an analysis of the electrostatic upper hybrid emissions at about 1315 SCET [*Kurth et al.*, 1987] using the relation $f_{UHR} = (f_p^2 + f_c^2)^{1/2}$ where f_{UHR} is the upper hybrid resonance frequency and f_c is the electron cyclotron frequency. The upper frequency limit of the radio emission is derived from the wideband data. The upper frequency cutoff suggests the density of the solar wind which forms the exterior wall of the cavity. This frequency (2–3 kHz) is consistent with the plasma frequency in the solar wind as derived from electron plasma oscillations observed prior to Voyager's crossing of the bow shock [*Gurnett et al.*, 1986].

Finally, it is important to point out in Figure 3 the existence of the intense, bursty emissions centered near 1300 SCET at 1 and 1.78 kHz. These have been identified by *Kurth et al.* [1987] as Bernstein emissions; the highest frequency of these Bernstein emissions is most likely the upper hybrid band [*Kurth et al.*, 1979]. As will be discussed below, the upper hybrid band is commonly believed to be the source of nonthermal continuum radiation in planetary magnetospheres [*Gurnett*, 1975; *Jones*, 1980; *Kurth et al.*, 1981].

As might be discerned by inspection of Figures 1–3, the 1- to 3-kHz emission extends low enough in frequency to be observed by the planetary radio astronomy receiver in its 1.2-kHz channel. The data for this channel are shown in Figure 4 for a time interval similar to that of Figure 3. Figure 4 shows the intensity and polarization of emission as a function of time by displaying the net polarized signal (RH − LH) so that the RH (LH) polarized emission is positive (negative). In the time interval of about 1008–1205 SCET the continuum radiation can clearly be seen as a right-hand polarized signal. The timing of this signal corresponds well to the emission observed by the plasma wave receiver. Given that the source of the waves is in the magnetic equator, it is straightforward to deduce the mode of propagation of the waves. At this time (prior to about 1315 SCET) the spacecraft is south of the magnetic equator; hence the wave vectors form an obtuse angle with respect to the magnetic field at the source. The observed right-hand polarization, then, implies that the waves are emitted in the ordinary (*L-O*) magnetoionic mode. This is the same mode as the bulk of the terrestrial continuum radiation [*Gurnett et al.*, 1988].

2.2. *Diffuse Emissions at Higher Frequencies*

In our search for the trapped continuum radiation discussed above, we found evidence for similar emissions at higher frequencies. These higher-frequency emissions showed frequency-time characteristics similar to the continuum radiation in that they showed little variation in intensity with either frequency or time. On the basis of the similarities, we are compelled to report on the higher-frequency observations and consider the possibility that they represent continuum rather than diffuse electrostatic emissions as reported earlier [*Kurth et al.*, 1987].

The first evidence of the higher-frequency component actually appears in Figures 1 and 2 above about 7 kHz. Apart from its frequency range, this higher-frequency emission appears to be very similar to the lower frequency band between 1 and 2.3 kHz. Another example of higher-frequency emissions similar to the continuum radiation is shown in Plate 3. This 10-s wideband interval was obtained at a distance of 10.4 R_U on the outbound leg, hence on the nightside of Uranus. The radio emission of interest is actually composed of at least two components, one being a relatively narrow band near 4 kHz and the other a more substantial component extending upward of 6 kHz. The gap near 7 kHz in the spectrum of the higher-frequency component could be an artifact of the notch filter at 7.2 kHz used to limit interference at the third harmonic of the spacecraft power supply. It is also possible that the band between 6 and 7 kHz is actually a separate component. In any case, the emission above 7 kHz is very similar to the high-frequency emission seen in Plate 1.

Figure 5 is a plot of spectral density as a function of frequency (on a linear frequency scale) for the interval shown in Plate 3. In this form it is easy to see the various components of the emission. It is clear here, as in Figure 1, that the $f > 7$ kHz component falls off in intensity with increasing frequency. As will be discussed below, this decrease in intensity with increasing frequency suggests that the emission is not related to more intense radio emissions at higher frequencies.

On the basis of a survey of all available wideband data at Uranus, the higher-frequency emission is almost always present in the magnetosphere within about 60 R_U except for those frames taken within 1–2 hours of closest approach when the whistler mode emission is quite intense [*Gurnett et al.*, 1986; *Coroniti et al.*, 1987]. For these times it is possible that the emission is present but swamped by the more intense whistler mode waves. It is also possible that the emissions are simply not present because of higher plasma frequencies in the inner magnetosphere.

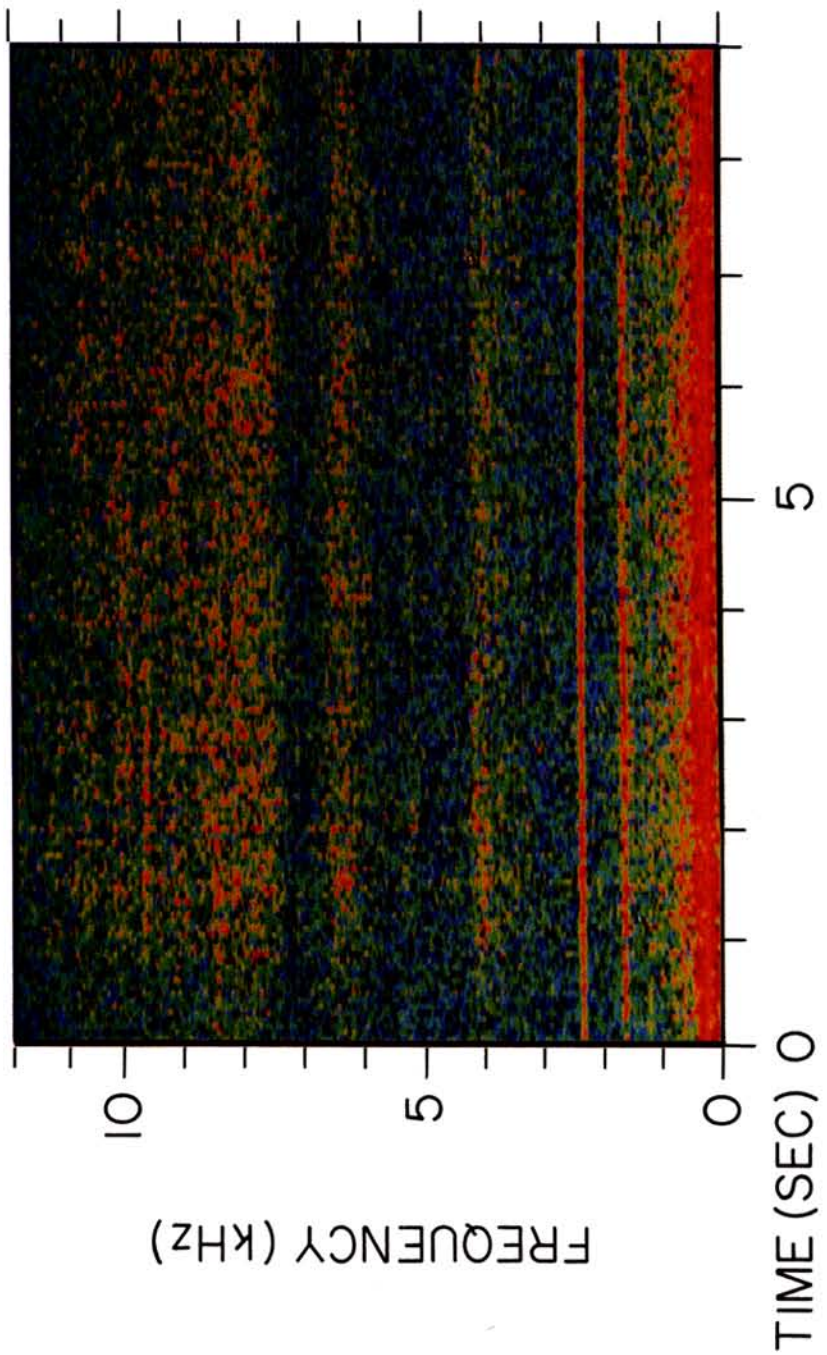

Plate 3. Example of diffuse emissions showing a complex spectrum observed on the outbound (nightside) leg of the encounter. The gap in the spectrum near 7 kHz could be due to a notch filter designed to limit interference from the third harmonic of the spacecraft power supply.

There is evidence of a diffuse emission in wideband data taken at 1858, 1920, and 1947 SCET extending down to about 8 kHz in the first two intervals and about 5 kHz in the third, and we must question whether these diffuse emissions are radio waves or not. In each case, the frequency of the diffuse noise is less than the electron plasma frequency suggested by the analysis of *Kurth et al.* [1987]; if the waves are radio waves propagating in a "free-space" mode, the profile of f_p of *Kurth et al.* [1987] is too high for these three periods. The example of 1920 SCET can be seen in Plate 1 of *Kurth et al.* [1987]. Kurth et al. identified an intense narrow-band emission in the example taken at 1920 SCET as the $3f_c/2$ Bernstein emission. That the diffuse emission of interest here is within the same gyroharmonic band as the $3f_c/2$ band suggests that the diffuse emission could be analogous to the diffuse electrostatic bands reported at the Earth by *Shaw and Gurnett* [1975]. As their name implies, the diffuse electrostatic bands are less well defined in frequency than the electrostatic electron cyclotron harmonic (ECH) emissions; the diffuse bands are also much weaker than the ECH emissions. Each emission, however, lies between harmonics of the electron cyclotron frequency. The diffuse noise seen at 1858 and 1947 SCET is also consistent with the diffuse electrostatic band interpretation. At 1947 SCET there is a local minimum in wave intensity near the second harmonic of f_c, suggesting that both the $3f_c/z$ and the $5f_c/z$ emissions are present. We suggest that the original profile for f_p of *Kurth et al.* [1987] is correct and the diffuse emissions observed between 1858 and 1947 SCET are diffuse electrostatic bands. However, it is not possible to totally resolve this point on the basis of the available data.

3. Discussion

In section 2.1 we presented evidence of a weak, diffuse emission which is propagating in the *L-O* mode within the low-density cavity formed in the outer magnetosphere on the dayside of Uranus. By analogy with terrestrial observations as well as those at Jupiter and Saturn, it seems quite reasonable to label this emission in the frequency range of 1–3 kHz as trapped nonthermal continuum radiation.

The generation mechanism for continuum radiation has long been associated with the intense upper hybrid resonance (UHR) bands [*Gurnett*, 1975; *Jones*, 1980; *Kurth et al.*, 1981]. Recently, evidence has been uncovered [*Jones et al.*, 1987; *Gurnett et al.*, 1988] that validates a linear mechanism for converting the electrostatic waves into electromagnetic waves via the so-called radio window theory [*Budden*, 1961; *Oya*, 1971; *Jones*, 1976; *Budden and Jones*, 1987]. The theory treats the propagation of electrostatic upper hybrid waves in the presence of a density gradient; given that the density gradient is approximately perpendicular to the magnetic field, the electrostatic waves can be transformed into electromagnetic *Z* mode waves which, in turn, can propagate through a radio window at the plasma frequency and escape as ordinary mode radiation [*Oya*, 1971; *Jones*, 1980, 1976]. *Jones* [1980] showed that the ordinary mode waves would propagate away from the source in beams that were directed at specific angles from the magnetic field based on the ratio of the electron plasma frequency to electron cyclotron frequency. The recent work of *Jones et al.* [1987] validated the beaming predictions of the theory, and that of *Gurnett et al.* [1988] showed that the polarization of the waves is as predicted by the theory for terrestrial examples. We see no evidence of beaming in the Uranus continuum radiation. However, this is to be expected if the emission is trapped in the magnetospheric cavity and suffers multiple reflections. The beaming predicted by the theory has only been observed at other planets in the escaping component.

On the basis of our knowledge of terrestrial continuum radiation and the accompanying theory, the source of the Uranian continuum emission is readily observable in the spectrum analyzer data shown in Figure 3 in the form of Bernstein waves at the upper hybrid resonance frequency. Figure 6 gives a schematic view of the origin of the low-frequency radio emissions. The upper hybrid waves are found between harmonics of the electron cyclotron frequency on the density gradient encountered as Voyager approached Uranus. That Voyager detected an upper hybrid band only near 1315 SCET at about 1.6 kHz [*Kurth et al.*, 1987] is only because these emissions are strongly confined to the magnetic equatorial plane. Had Voyager crossed the magnetic equator at different radial distances, it would almost certainly have detected other upper hybrid bands at different frequencies. It seems most reasonable to expect the

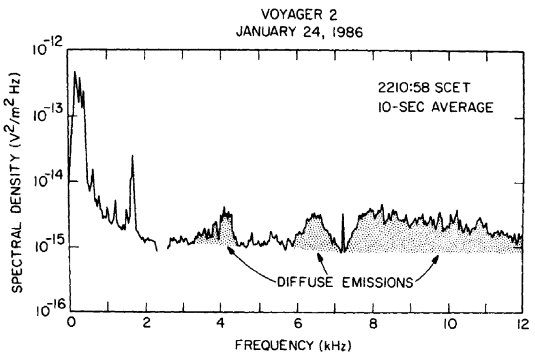

Fig. 5. Electric field spectral density spectrum showing the high-frequency diffuse emission which consists of at least two bands. Note that the intensity of the high-frequency band decreases with increasing frequency above 7 kHz.

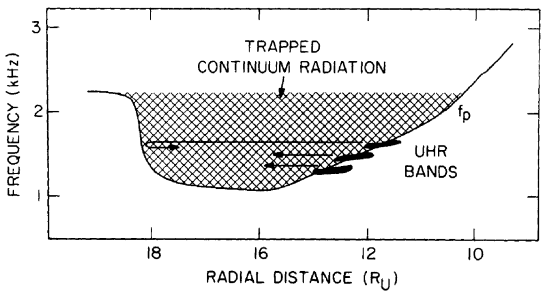

Fig. 6. Schematic drawing of the generation and trapping of the low-frequency continuum radiation in the dayside Uranian magnetosphere. The UHR bands are likely spread in frequency all along the density gradient leading to the inner magnetosphere; however, Voyager detected them only in a very narrow radial distance range limited by where the trajectory crossed the magnetic equatorial plane.

UHR bands to be present over a broad range of distances and frequencies.

In the case of Uranus (as at Saturn) the density cavity formed by the magnetosphere is not very deep; the dayside electron density is about 0.02 cm^{-3} (based on the continuum radiation cutoff) compared to about 0.05 cm^{-3} in the surrounding solar wind. At Jupiter the density deep in the tail lobes can be as low as about 10^{-5} cm^{-3} [*Gurnett et al.*, 1980; *Moses et al.*, 1987] compared to a solar wind density at 5 AU of about 0.4 cm^{-3}. *Gurnett* [1975] suggested that the intensity buildup of the continuum radiation inside the cavity was related to the Q of the cavity. Here we loosely define Q as being the number of times a wave will reflect at the wall of the cavity before being lost. Given that a shallow cavity would be more lossy than a deeper cavity and have a smaller Q, it follows that the Uranian continuum radiation should be relatively weak, as observed, for a given source strength. The very deep cavity at Jupiter is the primary example of a lossless or high-Q cavity; the intensities of continuum radiation there are up to 6 orders of magnitude more intense than at Uranus.

The importance of the existence of continuum radiation in the magnetosphere of Uranus is based on the ubiquity of the continuum radiation in planetary magnetospheres and the fact that a very broad range of plasma conditions can give rise to the radio emission. The characteristics of the plasma, its source(s), the magnetospheric energy source(s), and even the magnetospheric configuration vary widely between the Earth, Jupiter, Saturn, and Uranus, yet the emission manages to be produced in each magnetosphere. The fundamental conclusion is that the radio window mechanism producing continuum radiation must be included as a primary candidate in generating radio emissions from astrophysical sources along with other sources such as synchrotron emission and the cyclotron maser instability.

The nature of the higher-frequency diffuse emissions presented in section 2.2 must be considered very carefully. There are at least four possible interpretations for these emissions. First, it is possible that the higher-frequency component is simply a lower-frequency extension of a higher-frequency emission, such as the smooth, low-frequency emission observed by the planetary radio astronomy investigation [*Leblanc et al.*, 1987]. Second, the emissions could be related to the sporadic, narrow-band emissions reported by *Kurth et al.* [1986]. Third, the emissions could be identical to the low-frequency continuum radiation but simply have source upper hybrid bands at smaller radial distances and hence at higher frequencies than those related to the 1- to 3-kHz emission. Fourth, the higher-frequency waves could be a distinctly new radio emission with an as yet unknown generation mechanism different from that of the continuum radiation.

We have already argued against the first of the above options. The intensity of the $f > 7$ kHz emission decreases with increasing frequency; hence it is unlikely that the emission is the lower-frequency extension of one of the more dominant radio emissions already reported. The second option mentioned above refers to a continuum component sometimes observed in conjunction with the narrow-band bursty emissions near 5 kHz on the nightside of Uranus [*Kurth et al.*, 1986]. The fact that Kurth et al. concluded that the narrow-band emission is most likely generated by mode conversion from upper hybrid waves (as is continuum radiation) means the second and third options are basically the same. Hence a likely explanation for the higher-frequency emissions is that the radiation is generated in the same way as the trapped continuum radiation observed on the dayside between 1 and 3 kHz, except that the source upper hybrid waves lie closer to the planet and hence have higher frequencies. This solution also explains the additional component(s) seen in the example in Plate 3 and Figure 5. The separate emission bands could be related to sets of UHR emissions that are widely separated in location and frequency.

The only question raised by identifying the higher-frequency emission as continuum radiation has to do with the spectrally diffuse nature of the emission. Continuum radiation is typically generated in narrow bands [*Kurth*, 1982]; the low-frequency trapped component becomes diffuse because of the combined effects of multiple sources and Fermi-Compton scattering at the moving walls of the cavity [*Barbosa*, 1981]. For the higher-frequency emission, only the superposition of multiple sources works to smear a narrow-band spectrum into a diffuse one. In spite of being at frequencies high enough to escape from the magnetosphere, the higher-frequency component of continuum radiation appears as diffuse as the trapped component. The diffuse nature of the higher-frequency waves argues against the continuum radiation explanation. However, the remaining alternative for the higher-frequency waves is a distinctly new emission. We prefer to not "invent" yet another species of radio emissions at Uranus until there is a more convincing argument against the continuum explanation.

4. CONCLUSIONS

We have demonstrated the existence of classic, ordinary mode, trapped nonthermal continuum radiation in the dayside magnetosphere of Uranus, including likely candidate source waves in the form of upper hybrid resonance bands near $R = 12\ R_U$. The occurrence of this type of radio emission at Uranus is consistent with a ubiquitous generation mechanism which apparently exists in all planetary magnetospheres and suggests that the mechanism should be included as a primary candidate for astrophysical radio emissions along with other, more traditional mechanisms. The continuum radiation spectrum at Uranus is complex, consisting not only of the trapped component below about 3 kHz but also of one or more bands above about 4 kHz.

Acknowledgments. We acknowledge N. F. Ness and the Planetary Data System for the Voyager magnetometer measurements used in the calculation of electron cyclotron frequencies. This research was supported by the National Aeronautics and Space Administration through contract 957723 from the Jet Propulsion Laboratory.

The Editor thanks C. Sawyer and another referee for their assistance in evaluating this paper.

REFERENCES

Barbosa, D. D., Fermi-Compton scattering due to magnetopause surface fluctuations in Jupiter's magnetospheric cavity, *Astrophys. J.*, *243*, 1076, 1981.

Budden, K. G., *Radio Waves in the Ionosphere*, Cambridge University Press, New York, 1961.

Budden, K. G., and D. Jones, Conversion of electrostatic upper hybrid emissions to electromagnetic O and X mode waves in the Earth's magnetosphere, *Ann. Geophys., Ser. A*, *5*, 21, 1987.

Coroniti, F. V., W. S. Kurth, F. L. Scarf, S. M. Krimigis, C. F.

Kennel, and D. A. Gurnett, Whistler mode emissions in the Uranian radiation belts, *J. Geophys. Res.*, *92*, 15,234, 1987.
Desch, M. D., and M. L. Kaiser, Ordinary mode radio emission from Uranus, *J. Geophys. Res.*, *92*, 15,211, 1987.
Gurnett, D. A., The Earth as a radio source: The nonthermal continuum, *J. Geophys. Res.*, *80*, 2751, 1975.
Gurnett, D. A., W. S. Kurth, and F. L. Scarf, The structure of the Jovian magnetotail from plasma wave observations, *Geophys. Res. Lett.*, *7*, 53, 1980.
Gurnett, D. A., W. S. Kurth, F. L. Scarf, and R. L. Poynter, First plasma wave observations at Uranus, *Science*, *233*, 106, 1986.
Gurnett, D. A., W. Calvert, R. L. Huff, D. Jones, and M. Sugiura, The polarization of escaping terrestrial continuum radiation, *J. Geophys. Res.*, *93*, 12,817, 1988.
Jones, D., Source of terrestrial nonthermal radiation, *Nature*, *260*, 686, 1976.
Jones, D., Latitudinal beaming of planetary radio emissions, *Nature*, *288*, 225, 1980.
Jones, D., W. Calvert, D. A. Gurnett, and R. L. Huff, Observed beaming of terrestrial myriametric radiation, *Nature*, *328*, 391, 1987.
Kraus, J. D., *Radio Astronomy*, McGraw-Hill, New York, 1966.
Kurth, W. S., Detailed observations of the source of terrestrial narrowband electromagnetic radiation, *Geophys. Res. Lett.*, *9*, 1341, 1982.
Kurth, W. S., J. D. Craven, L. A. Frank, and D. A. Gurnett, Intense electrostatic waves near the upper hybrid resonance frequency, *J. Geophys. Res.*, *84*, 4145, 1979.
Kurth, W. S., D. A. Gurnett, and R. R. Anderson, Escaping nonthermal continuum radiation, *J. Geophys. Res.*, *86*, 5519, 1981.
Kurth, W. S., F. L. Scarf, J. D. Sullivan, and D. A. Gurnett, Detection of nonthermal continuum radiation in Saturn's magnetosphere, *Geophys. Res. Lett.*, *9*, 889, 1982.
Kurth, W. S., D. A. Gurnett, and F. L. Scarf, Sporadic narrow-band radio emissions from Uranus, *J. Geophys. Res.*, *91*, 11,958, 1986.
Kurth, W. S., D. D. Barbosa, D. A. Gurnett, and F. L. Scarf, Electrostatic waves in the magnetosphere of Uranus, *J. Geophys. Res.*, *92*, 15,225, 1987.
Leblanc, Y., M. G. Aubier, A. Ortega-Molina, and A. Lecacheux, Overview of the Uranian radio emissions: Polarization and constraints on source locations, *J. Geophys. Res.*, *92*, 15,125, 1987.
Moses, S. L., W. S. Kurth, C. F. Kennel, F. V. Coroniti, and F. L. Scarf, Polarization of low-frequency electromagnetic radiation in the lobes of Jupiter's magnetotail, *J. Geophys. Res.*, *92*, 4701, 1987.
Oya, H., Conversion of electrostatic plasma waves into electromagnetic waves: Numerical calculation of the dispersion relation for all wavelengths, *Radio Sci.*, *6*, 1131, 1971.
Scarf, F. L., and D. A. Gurnett, A plasma wave investigation for the Voyager mission, *Space Sci. Rev.*, *21*, 289, 1977.
Scarf, F. L., D. A. Gurnett, and W. S. Kurth, Jupiter plasma wave observations: An initial Voyager 1 overview, *Science*, *204*, 991, 1979.
Shaw, R. R., and D. A. Gurnett, Electrostatic noise bands associated with the electron gyrofrequency and plasma frequency in the outer magnetosphere, *J. Geophys. Res.*, *80*, 4259, 1975.
Sittler, E. C., Jr., K. W. Ogilvie, and R. Selesnick, Survey of electrons in the Uranian magnetosphere: Voyager 2 observations, *J. Geophys. Res.*, *92*, 15,263, 1987.
Warwick, J. W., J. B. Pearce, R. G. Peltzer, and A. C. Riddle, Planetary radio astronomy experiment for Voyager missions, *Space Sci. Rev.*, *21*, 309, 1977.
Warwick, J. W., et al., Voyager 2 radio observations of Uranus, *Science*, *233*, 102, 1986.

M. D. Desch, Code 695, NASA Goddard Space Flight Center, Greenbelt, MD 20771.
D. A. Gurnett and W. S. Kurth, Department of Physics and Astronomy, University of Iowa, Iowa City, IA 52242.

(Received February 9, 1989;
revised April 24, 1989;
accepted April 26, 1989.)